

# Predefined-time synchronization of 5D Hindmarsh–Rose neuron networks via backstepping design and application in secure communication

Lin, Lixiong

**Predefined-time synchronization of 5D Hindmarsh–Rose neuron networks via backstepping design and application in secure communication**

Nonlinear Analysis: Modelling and Control, vol. 27, núm. 4, 2022

Vilniaus Universitetas, Lituania

**Disponible en:** <https://www.redalyc.org/articulo.oa?id=694173183002>

**DOI:** <https://doi.org/10.15388/namc.2022.27.26557>




Esta obra está bajo una Licencia Creative Commons Atribución-NoComercial-SinDerivar 4.0 Internacional.

# Predefined-time synchronization of 5D Hindmarsh–Rose neuron networks via backstepping design and application in secure communication

Lixiong Lin [elelinlixiong@139.com](mailto:elelinlixiong@139.com)

*Jimei University, China*

 <https://orcid.org/0000-0002-9829-5358>

Nonlinear Analysis: Modelling and Control, vol. 27, núm. 4, 2022

Vilniaus Universitetas, Lituania

Recepción: 13 Mayo 2021

Publicación: 13 Abril 2022

DOI: <https://doi.org/10.15388/namc.2022.27.26557>

Redalyc: <https://www.redalyc.org/articulo.oa?id=694173183002>

**Abstract:** In this paper, the fast synchronization problem of 5D Hindmarsh–Rose neuron networks is studied. Firstly, the global predefined-time stability of a class of nonlinear dynamical systems is investigated under the complete beta function. Then an active controller via backstepping design is proposed to achieve predefined-time synchronization of two 5D Hindmarsh–Rose neuron networks in which the synchronization time of each state variable of the master-slave 5D Hindmarsh–Rose neuron networks is different and can be defined in advance, respectively. To show the applicability of the obtained theoretical results, the designed predefined-time backstepping controller is applied to secure communication to realize asynchronous communication of multiple different messages. Three numerical simulations are provided to validate the theoretical results.

**Keywords:** 5D Hindmarsh–Rose neuron networks, predefined-time stability, complete beta function, secure communication.

## Introduction

The fast synchronization problem of nonlinear systems has attracted much attention in recent years [1, 2, 4, 32, 33], e.g., finite-time synchronization problem for two nonlinear systems. The primary purpose of finite-time synchronization is to design an appropriate controller to achieve the master-slave systems coupled within a finite time interval [3]. Ahmad et al. [4] proposed an active controller to realize finite-time multi-switching synchronization of chaotic systems. The initial condition of the nonlinear systems will affect the settling time of finite-time synchronization. If the initial condition of the systems is unknown, the settling time of finite-time synchronization cannot be obtained in advance. To solve the above problem, fixed-time stability was proposed by [25] and applied to fixed-time synchronization. Different from finite-time synchronization, fixed-time synchronization has a definite synchronization settling time [8, 14–16]. Hu et al. [12] proposed a fixed-time stability theorem. The proposed approach shows better performance than [25]. Kong et al. [16] investigated the fixed-time synchronization of discontinuous fuzzy inertial neural networks with parameter uncertainties. Then Kong et al. [14] further investigated the fixed-time synchronization of discontinuous fuzzy inertial neural

networks with time varying delays. Chen et al. [7] reconstructed the Lyapunov function and reproved the fixed-time stability theorem through inequalities, and its settling time was further improved. Lin et al. [19] proposed a new fixed-time stability theorem and proved that the settling time is more accurate estimation by segmenting the Lyapunov function. Many studies on the settling time estimation are based on inequality theories. How to improve the accuracy of the settling time estimation of fixed-time stability is still a direction for further research.

In practical applications, such as secure communications or multiple agents control systems, it is hoped that in the controller design stage, the least upper bound of the settling time can be set as a tuning parameter of the system. Fixed-time stability is difficult to establish a direct relationship between the upper bound of the settling time and the parameters of nonlinear system. In order to solve the above-mentioned difficulties, a new kind of time stability, named predefined-time stability, was introduced in [27]. The research on predefined-time stability is still in the initial stage [13, 22, 26]. Muñoz-Vázquez et al. [24] proposed an active predefined-time controller to achieve synchronization between two coupled Lorenz systems and applied to secure communication. To enable fully exact tracking of actuated mechanical systems, an predefined-time controller was proposed to second-order systems in [23]. Predefined-time stability theorems can realize that all variables of the nonlinear system are stable within a predefined time. In secure communication, different messages are of different importance, and the transmission sequence is also different. Therefore, it is very necessary to design an active control algorithm to achieve different settling time for different variables, so as to achieve asynchronous time synchronization of multiple messages communications.

In data encryption and secure communication, there are three very important factors:

(i) complexity of the dynamical nonlinear system; (ii) short transmission response time; fast synchronization. These factors can increase the difficulty of hackers to crack. The one-dimensional chaotic system has simple model, easy circuit implementation, and relatively simple synchronization, but its output only has one state, which is not conducive to confidentiality. Therefore, chaotic systems with relatively high dimension are generally considered in secure communication. The 2D Hindmarsh–Rose (HR) chaotic system has attracted much attention because of its fast computational speed [10], which is more than ten times faster than the Hodgkin and Huxley model [11], and complex dynamical behaviors, such as bursting and chaos, observed in real biological neurons. Many researches have been conducted on the HR neural chaotic systems [21, 28, 29, 31], and the HR neural chaotic systems have been extended to 3D HR neural chaotic systems [28], 4D HR neural chaotic systems [21], and even 5D HR neuron networks (5D HRNNs) [31]. The rich dynamical behaviors, including a chaotic super-bursting regime, of the 5D HRNN was shown in [31], and the synchronization of two coupled 5D HR neuron networks was realized. Therefore, the 5D HRNN

is particularly suitable for the field of secure communication. At present, the research on the synchronization of the HR neuron network mainly focuses on asymptotically stable [5,20,30], the research on the fixed-time synchronization of the HRNNs has not been seen yet. Inspired by the above discussions, predefined-time synchronization of two 5D HRNNs via backstepping design is proposed in this paper. The main contribution are the following:

To solve the problem of inaccurate estimation of the settling time, this paper introduces complete beta function to achieve accurate settling time estimation of the predefined-time stability.

An active controller via backstepping design is proposed to achieve the predefined- time synchronization of master-slave 5D HRNNs in which the synchronization time of each state variable of the master-slave 5D HRNNs is different and can be defined in advance, respectively. The designed controller is applied to secure communication to realize asynchronous communication of multiple messages.

(i) To solve the problem of inaccurate estimation of the settling time, this paper introduces complete beta function to achieve accurate settling time estimation of the predefined-time stability.

(ii) An active controller via backstepping design is proposed to achieve the predefined- time synchronization of master-slave 5D HRNNs in which the synchronization time of each state variable of the master-slave 5D HRNNs is different and can be defined in advance, respectively. The designed controller is applied to secure communication to realize asynchronous communication of multiple messages.

The remainder of this paper is structured as follows. Some preliminaries are included in Section 2. In Section 3, a new predefined-time stability of a class of nonlinear systems is investigated under the complete beta function. With the help of predefined-time stability, the predefined-time synchronization of master-slave 5D HRNNs via backstepping design is investigated in Section 4. Then the designed predefined-time backstepping controller is applied to secure communication in Section 5. The conclusion is given in Section 6.

## 2 Preliminaries

Consider a nonlinear system described by the following [18]:

$$\dot{x} = f(x; r),$$

where  $x \in \mathbb{R}^n$  is the state vector of system (1).  $x_0$  is the initial condition.  $r \in \mathbb{R}^b$  with  $r \in \mathbb{R}^b$  is the parameters  $f: \mathbb{R}^n \rightarrow \mathbb{R}^n$  is a nonlinear function

the process of deriving fixed-time stability, the complete beta function and complete gamma function will play a key role. The definition of these functions will be provided the following.

**Definition 1.** (See [9].) Let  $B(\sigma, \theta)$ . The complete beta function, denoted by  $B(\sigma, \theta)$ , is defined by the Euler integral and the complete gamma function through

$$B(\sigma, \theta) = \int_0^1 z^{\sigma-1} (1-z)^{\theta-1} dz = \frac{\Gamma(\sigma)\Gamma(\theta)}{\Gamma(\sigma+\theta)},$$

where  $\Gamma(\cdot)$  is the complete gamma function, which is defined by the Euler integral  $\Gamma(z) = \int_0^\infty e^{-t} t^{z-1} dt$ .

The complete beta function is mainly used in statistics, but it is also used in other fields, e.g., actuarial science, economics or telecommunications. In this paper, we apply it to fixed-time stability.

**Definition 2.** (See [25].) The origin of system (1) is globally fixed-time stable if it is globally finite-time stable and the settling time is bounded, i.e., there exists  $T_{\max} > 0$  such that, for all  $x_0 \in \mathbb{R}^n$ ,  $T(x_0) \leq T_{\max}$ .

**Definition 3.** (See [19].) The origin of system (1) is said to be predefined-time stable if it is globally fixed-time stable and the settling time  $T(x_0)$  is

$$T(x_0) \leq T_c \quad \forall x_0 \in \mathbb{R}^n,$$

where  $T_c$  is a tuning constant parameter and called a predefined time.

**Lemma 1.** (See [6].) For system (1), let there exist a continuous radially unbounded and positive definite function  $V(x) : \mathbb{R}^n \rightarrow \mathbb{R}$  and  $\delta > 0$ ,  $0 < \kappa < 1$  such that

$$\dot{V}(x) \leq -\delta V^\kappa(x) \quad \forall t \geq t_0 \text{ and } V(x(t_0)) \geq 0,$$

where  $t_0$  is the any initial time;  $x(t_0)$  is the any initial value. Then the relationship between time  $t$  and  $V(x(t))$  is described as

$$t = \frac{V^{1-\kappa}(x(t_0))}{\delta(1-\kappa)} + t_0,$$

and system (1) is finite-time stable

**Lemma 2.** (See [12].) For system (1), let there exist a continuous radially unbounded and positive definite function  $V(x) : \mathbb{R}^n \rightarrow \mathbb{R}$  and  $\alpha, \beta, \gamma, \eta > 0$  satisfying  $\gamma\eta > 1$  such that

$$\dot{V}(x) \leq -(\alpha V^\gamma(x) + \beta)^\eta, \quad x(t) \in \mathbb{R}^n \setminus \{0\}.$$

Then system (1) can converge to the zero in the settling time  $T_{\max}^{\alpha, \beta}$  and  $T_{\max}^{\gamma, \eta}$  is described

$$T(x_0) \leq T_{\max}^1 \triangleq \frac{1}{\beta^\eta} \left( \frac{\beta}{\alpha} \right)^{1/\gamma} \left( 1 + \frac{1}{\gamma\eta - 1} \right).$$

**Lemma 3.** (See [24].) For system (1), let there exist a continuous radially unbounded and positive definite function  $V(x) : \mathbb{R}^n \rightarrow \mathbb{R}$  and  $0 < \mu < 1$  such that

$$\dot{V}(x) \leq -\frac{\pi}{2\mu T_c} (V^{1-\mu}(x) + V^{1+\mu}(x)).$$

Then system (1) is globally predefined-time stable, and the predefined time is  $r_c$ .

**Lemma 4.** (See [17].) If conditions satisfy  $x_1, x_2, \dots, x_n \geq 0, 0 < \epsilon_1 \leq 1, \epsilon_2 > 1$ , then

$$\sum_{i=1}^n x_i^{\epsilon_1} \geq \left( \sum_{i=1}^n x_i \right)^{\epsilon_1}, \quad \sum_{i=1}^n x_i^{\epsilon_2} \geq n^{1-\epsilon_2} \left( \sum_{i=1}^n x_i \right)^{\epsilon_2}.$$

### 3 Predefined-time stability

The goal of this section is to propose a new fixed-time stability proof method for system (1). By making some modification of the fixed-time system, a new predefined-time stability theorem is proposed.

**Theorem 1.** For system (1), if there exist a continuous radially unbounded and positive definite function  $V(x) : \mathbb{R}^n \rightarrow \mathbb{R}$  and  $\alpha, \beta, \gamma, \eta > 0$ , satisfying  $\gamma\eta > 1$  such that

$$\dot{V}(x) \leq -(\alpha V^\gamma(x)^\gamma + \beta)^\eta,$$

then system (1) is globally fixed-time stable with the settling time

$$T(x_0) \leq T_{\max}^2 = \frac{\beta^{1/\gamma-\eta}}{\alpha^{1/\gamma\gamma}} B(\sigma, \theta),$$

where  $B(\sigma, \theta)$  is the complete beta function.

**Proof.** Since  $\alpha, \beta > 0$ , then

$$\frac{dV(x)}{dt} \leq -(\alpha V^\gamma(x)^\gamma + \beta)^\eta \leq -\beta^\eta < 0.$$

Since  $dV(x)/dt \leq -\beta^\eta$ , there exists a constant  $T(x_0) = V(x_0)/\beta^\eta$  such that  $\lim_{t \rightarrow T(x_0)} V(x) = 0$  and  $V(x) = 0$  for all  $t > T(x_0)$ . It follows that  $dV(x) \leq -dt$ , then

$\frac{dV(x)}{(\alpha V^\gamma(x)^\gamma + \beta)^\eta} \leq -dt$  then  $\frac{dV(x)}{(\alpha V^\gamma(x)^\gamma + \beta)^\eta} \leq -dt$ .

We have

$$\begin{aligned}\nabla^{n-1}\sigma(k) &= f(x(k), u(k)), \\ \nabla z(\omega, k) &= -\omega z(\omega, k) + \sigma(k), \\ x(k) &= \int_0^{+\infty} \mu_{\alpha-n+1}(\omega) z(\omega, k) d\omega, \\ y(k) &= g(x(k), u(k)),\end{aligned}$$

Let  $z = ((\alpha/\beta)V^\gamma + 1)^{-1}$  then  $z$  goes to 1 when and to 0 then  $V \rightarrow +\infty$ ,

$$V = \left( \frac{\beta}{\alpha} \left( \frac{1}{z} - 1 \right) \right)^{1/\gamma}$$

and

$$dV = -\frac{(\frac{\beta}{\alpha})^{1/\gamma}}{z^{2\gamma}} \left( \frac{1}{z} - 1 \right)^{1/\gamma-1} dz.$$

Thus formula (4) can be written as

$$\begin{aligned}\int_0^{+\infty} \frac{\beta^{-\eta}}{(\frac{\alpha}{\beta}V^\gamma + 1)^\eta} dV &= -\int_1^0 \frac{\beta^{-\eta}}{(\frac{\alpha}{\beta}\frac{\beta}{\alpha}(\frac{1}{z}-1) + 1)^\eta} \cdot \frac{(\frac{\beta}{\alpha})^{1/\gamma}}{z^{2\gamma}} \cdot \left( \frac{1}{z} - 1 \right)^{1/\gamma-1} dz \\ &= -\int_1^0 \beta^{-\eta} z^\eta \cdot \frac{(\frac{\beta}{\alpha})^{1/\gamma} (\frac{1}{z} - 1)^{1/\gamma-1}}{z^{2\gamma}} dz \\ &= -\frac{(\frac{\beta}{\alpha})^{1/\gamma}}{\beta^\eta \gamma} \cdot \int_1^0 z^{\eta-2} \cdot \frac{(1-z)^{1/\gamma-1}}{z^{1/\gamma-1}} dz \\ &= \frac{(\frac{\beta}{\alpha})^{1/\gamma}}{\beta^\eta \gamma} \cdot \int_0^1 z^{\eta-1-1/\gamma} \cdot (1-z)^{1/\gamma-1} dz.\end{aligned}$$

Assume  $\sigma = 1/\gamma$  and  $\theta - 1 = \eta - 1 - 1/\gamma$ , then

$$B(\sigma, \theta) = \int_0^1 z^{\sigma-1} (1-z)^{\theta-1} dz = \frac{\Gamma(\sigma)\Gamma(\theta)}{\Gamma(\sigma+\theta)},$$

Assume  $\sigma = 1/\gamma$  and  $\theta - 1 = \eta - 1 - 1/\gamma$ , then



$$B(\sigma, \theta) = \int_0^1 z^{\sigma-1} (1-z)^{\theta-1} dz = \frac{\Gamma(\sigma)\Gamma(\theta)}{\Gamma(\sigma+\theta)},$$

and formula (4) can be written as

$$T(x_0) \leq \int_0^{+\infty} \frac{\beta^{-\eta} dV}{(\frac{\alpha}{\beta} V^\gamma + 1)^\eta} = \frac{(\frac{\beta}{\alpha})^{1/\gamma}}{\beta^\eta \gamma} \cdot B(\sigma, \theta) = T_{\max}^2. \quad (5)$$

By Definition 2, systems (1) is fixed-time stable, and the settling time  $T_{\max}^2$  is bounded. Importar imagen for any, which completes the proof

**Remark 1.** Obviously, Theorem 1 provides a new proof process of fixed-time stability. Although Lyapunov function (3) is the same as that in [12] and [19], different settling time is obtained in Theorem 1. In the proof of Theorem 1, complete beta function is applied for the first time to realize the accurate settling time estimation, and a small upper bound of the settling time is obtained, closer to the real value.

**Theorem 2.** The settling time  $T_{\max}^2$  in Theorem 1 is more accurate than the settling time  $T_{\max}^1$  in Lemma

*Proof.* From the derivation process of Lemma 2 in [12] we have

$$T_{\max}^1 - T(x_0) \geq T_{\max}^1 - \int_0^{+\infty} \frac{1}{(\alpha V^\gamma + \beta)^\eta} dV \geq 0,$$

and from formula (5) we have

$$T_{\max}^2 = \int_0^{+\infty} \frac{1}{(\alpha V^\gamma + \beta)^\eta} dV,$$

then

$$T_{\max}^1 \geq T_{\max}^2.$$

That means the settling time  $T_{\max}^2$  is closer to the real convergence time than  $T_{\max}^1$ . This proof is completed.

Next, using the results obtained in Theorem 1, a new predefined-time stability is derived for a Lyapunov like condition.

**Theorem 3.** For system (1), let there exists a continuous radially unbounded and positive definite function  $V: \mathbb{R}^n \rightarrow \mathbb{R}$  such that any solution  $x(t, x_0)$  of system (1) satisfies



$$\dot{V} \leq -\frac{T_{\max}^2}{T_c} (\alpha V^\gamma + \beta)^\eta, \quad (6)$$

where  $\alpha, \beta, \gamma, \eta > 0$ ,  $\gamma\eta > 1$ , and  $T_{\max}^2$  are given in Theorem 1. Then system (1) is globally predefined-time stable, and the strong predefined time is  $T_c$ .

Proof. According to the supposing of Theorem 3, one has that

$$\begin{aligned} T(x_0) &= \int_0^{T(x_0)} dt \leq - \int_{+\infty}^0 \frac{T_c}{T_{\max}^2} \frac{1}{(\alpha V^\gamma + \beta)^\eta} dV \\ &= \int_0^{+\infty} \frac{T_c}{T_{\max}^2} \frac{1}{(\alpha V^\gamma + \beta)^\eta} dV = \int_0^{+\infty} \frac{T_c}{T_{\max}^2} \frac{\beta^{-\eta}}{(\frac{\alpha}{\beta} V^\gamma + 1)^\eta} dV \\ &= \frac{T_c}{T_{\max}^2} \int_0^{+\infty} \frac{\beta^{-\eta} dV}{(\frac{\alpha}{\beta} V^\gamma + 1)^\eta} = \frac{T_c}{T_{\max}^2} \frac{(\frac{\beta}{\alpha})^{1/\gamma}}{\beta^{\eta\gamma}} \cdot B(\delta, \theta) = T_c, \end{aligned}$$

where  $T_c$  is a tunable parameter of system (1). Consequently, system (1) is predefined-time stable, and the predefined time is  $T_c$ .

**Remark 2.** Compared with Lemma 1, Lyapunov function (6) in Theorem 3 has one more constant  $\beta$  and one more adjustable parameter  $T_c$ , which turn the asymptotically stability of Lemma 1 into predefined-time stability of Theorem 3.

**Remark 3.**  $T_{\max}^2$  is related to  $\alpha, \beta$ , and  $B(\delta, \theta)$ . If  $T_{\max}^2$  is to be adjusted, complicated calculation is needed. Compared with Theorem 1, Lyapunov function (6) in Theorem 3 has one more adjustable parameter  $T_c$ . The complex relationship between the system parameters and the settling time is transformed into an one-to-one correspondence between the settling time and the parameter  $T_c$ . By tuning  $T_c$ , system (1) can be stabilized at different predefined time, which is simpler and more effective than the fixed-time stability.

Example 1. Consider the following system:

$$\dot{y}(t) = -\text{sign}(y(t)) \cdot (\alpha |y(t)|^\gamma + \beta)^\eta,$$

where  $y(t)$  is a state variable, and the constants  $\alpha, \beta, \gamma, \eta > 0$  and  $\gamma\eta > 1$  satisfy the requirements of Theorem 1. Hence, system (7) is fixed-time stability by Theorem 1. In order to verify the validity of the Theorem 1, several sets of different parameters are simulated for system (7). The simulation results are given in Fig. 1 in which two sets of different parameters are chosen: (i)  $\alpha = 1.2$ ,  $\beta = 0.9$ ,  $\gamma = 4/7$ ,  $\eta = 5/2$ ; (ii)  $\alpha = 5$ ,  $\beta = 2$ ,  $\gamma = 2$ ,  $\eta = 0.9$ . By computation  $T_{\max}^1 = 2.6220$  s,  $T_{\max}^2 = 1.1662$  s, under the first set of parameters, and  $T_{\max}^1 = 0.7626$  s,  $T_{\max}^2 = 0.6235$  s under the second set of parameters, which shows that the estimation of the settling time

in Theorem 1 are more accurate compared with Lemma 2 and proves Theorem 2. Consider the following system:

$$\dot{y}(t) = -\frac{C_v}{T_c} \cdot \text{sign}(y(t)) \cdot (\alpha|y(t)|^\gamma + \beta_1 + d_{\text{dis}})^\eta,$$

where  $|d_{\text{dis}}| < D$  with According to Theorem 3, system (8) is predefined-time stable. In Fig. 2, system (8) converges to zero before a predefined time  $T_c$  for several different initial conditions, which is explicitly defined in advance; the simulation results are shown in Fig. 2(a) with  $T_c = 0.8$  s and Fig. 2(b) with  $T_c = 0.2$  s. Consider the following system:

$$\dot{y}(t) = -\frac{C_v}{T_c} \cdot \text{sign}(y(t)) \cdot (\alpha|y(t)|^\gamma + \beta_1 + d_{\text{dis}})^\eta, \quad (8)$$

According to Lemma 1, system (9) is finite-time stable. Figure 3 shows the comparative results of systems (8) and (9). From Fig. 3(a) the convergence time of systems (8) and (9) changes with different initial conditions. When the initial value is  $y(0) = 80$ , the convergence time of system (9) is 12 s, which exceeds the predefined time  $T_c = 10$  s. The convergence time of system (8) is less than  $T_c = 10$  s under any initial condition. Compared with system (9), the convergence time of system (8) can be estimated in advance without initial condition known. If the initial conditions are known, by setting different parameters, the convergence time of system (9) can be estimated in advance. The simulation results are shown in Fig. 3(b) in which the parameters are chosen:  $y(0) = 4$ ,  $\delta = 21.1336$  with  $T_c = 0.2$  s,  $\delta = 8.4534$  with  $T_c = 0.5$  s,  $\delta = 5.2834$  with  $T_c = 0.8$  s. From Fig. 3(b) system (9) can achieve more accurate settling time estimation if the initial conditions are known. Consider the following system:

$$\dot{y}(t) = -\frac{\pi}{2\mu T_c} \cdot \text{sign}(y(t)) \cdot (\alpha|y(t)|^{1-\mu} + \beta|y(t)|^{1+\mu} + d_{\text{dis}}). \quad [10]$$

According to Lemma 3, system (10) is predefined-time stable. Figure 4 shows the comparative results of systems (8) and (10) with disturbance occurring. It can be seen from Fig. 4 that Theorem 3 can effectively suppress disturbance and has better robustness than Lemma 3.

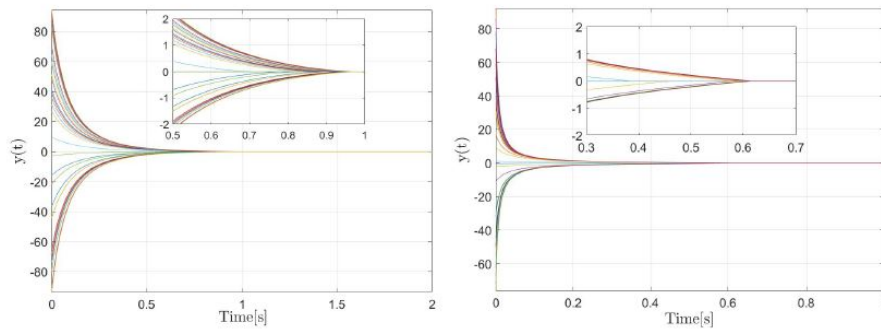


**Figure 1.** Trajectories of (7) for different initial conditions.

(a)  $\alpha = 1.2, \beta = 0.9, \gamma = 4/7, \eta = 5/2$

(b)  $\alpha = 5, \beta = 2, \gamma = 2, \eta = 0.9$

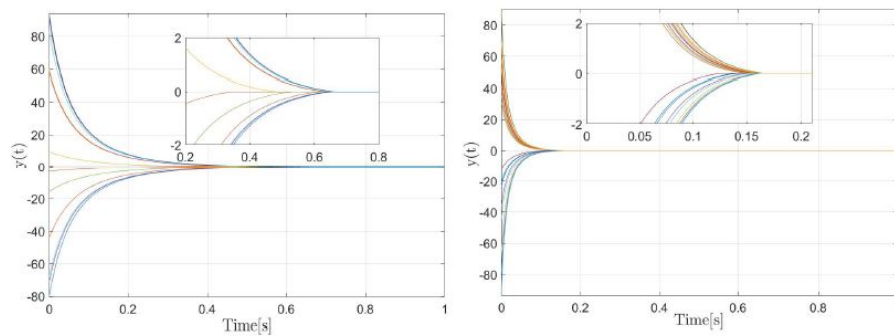


**Figure 2.** Trajectories of (8) for different initial conditions and the parameters

(a)  $T_c = 0.8 \text{ s}$

(b)  $T_c = 0.2 \text{ s}$

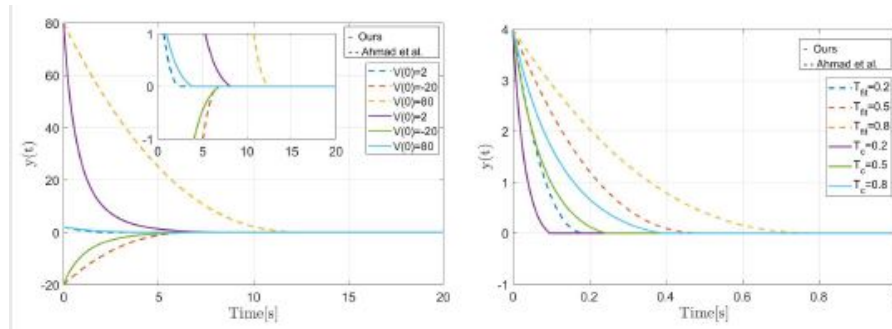


**Figure 3.** Comparative results of systems (8) and (9).

(a)  $T_c = 10 \text{ s}$

(b) Different  $T_c$

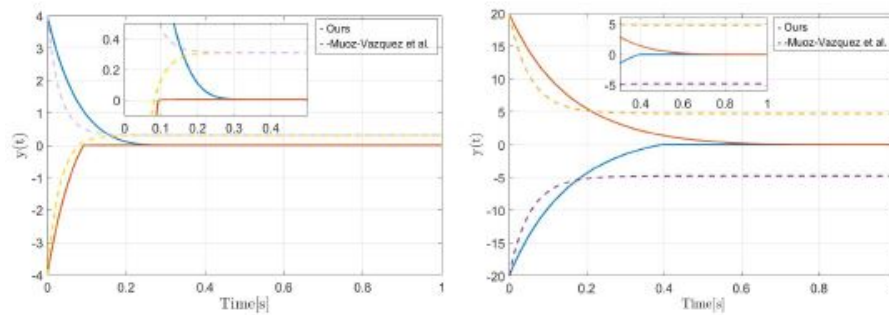


Figure 4. Comparative results of systems (8) and (10).

(a)  $y(0) = \pm 4, d_{\text{dis}} = 0.9$

(b)  $y(0) = \pm 20, d_{\text{dis}} = 0.9$

#### 4 Predefined-time synchronization controller via backstepping design

In this section, we will apply the theorems obtained in Section 3 and apply them to the predefined-time synchronization of master-slave 5D HRNNs via backstepping design. The 5D HRNN is described by

$$\begin{aligned}\dot{x}_1 &= -ax_1^3 + bx_1^2 + x_2 - cx_3 \\ &\quad + I_0 \cos(\Omega t - \psi) - k_1(d + 3sx_5^2)x_1, \\ \dot{x}_2 &= f - gx_1^2 - |x_2 - hx_4 + d_{\text{dis}}|, \\ \dot{x}_3 &= l[m(x_1 + x_{10}) - x_3], \\ \dot{x}_4 &= n[p(x_2 + x_{20}) - qx_4], \\ \dot{x}_5 &= x_1 - k_2x_5,\end{aligned}\tag{11}$$

where  $z(\omega, a) = 0$  is the membrane potential variable  $0 < \alpha < 1$  to  $n-1 < \bar{\alpha} < n$ , is the recovery current variable, which also is called spiking variable associated with fast ions,  $0 < \alpha < 1$  to  $n-1 < \bar{\alpha} < n$ , is the adaptation variable associated with slow ions,  $0 < \alpha < 1$  to  $n-1 < \bar{\alpha} < n$ , is an even slower process.  $0 < \alpha < 1$  to  $n-1 < \bar{\alpha} < n$ , is the magnetic flux across the neuron's cell membrane.  $0 < \alpha < 1$  to  $n-1 < \bar{\alpha} < n$ , is the amplitude of a harmonic stimulus with frequency and phase  $0 < \alpha < 1$  to  $n-1 < \bar{\alpha} < n$ , are the constant parameters. In neuron activity, the parameters  $n < l \ll 1$  play a very important role;  $l$  is the ratio of time scales between fast and slow fluxes across the neuron's membrane.  $n$  controls the speed change of a slower dynamical process, in particular, the calcium exchange between intracellular warehouse and the cytoplasm [21].  $j^{\text{dis}} < D$  is the disturbance. Let (11)

Let (11) be the master 5D HRNN, and the slave 5D HRNN is given by

$$\begin{aligned}\dot{\hat{x}}_1 &= -a\hat{x}_1^3 + b\hat{x}_1^2 + \hat{x}_2 - c\hat{x}_3 \\ &\quad + I_0 \cos(\Omega t - \psi) - k_1(d + 3s\hat{x}_5^2)\hat{x}_1 + u_1, \\ \dot{\hat{x}}_2 &= f - g\hat{x}_1^2 - \hat{x}_2 - h\hat{x}_4 + u_2,\end{aligned}\tag{121}$$

$$\begin{aligned}\dot{\hat{x}}_3 &= l[m(\hat{x}_1 + x_{10}) - \hat{x}_3] + u_3, \\ \dot{\hat{x}}_4 &= n[p(\hat{x}_2 + x_{20}) - q\hat{x}_4] + u_4, \\ \dot{\hat{x}}_5 &= \hat{x}_1 - k_2\hat{x}_5 + u_5,\end{aligned}\tag{122}$$

$i = 1; 2; \dots; 5$ , where  $\hat{x}_i \in \mathbb{R}$  represents the membrane potential variable;  $u_i$  is an activecontroller to be designed to achieve the predefined-time synchronization of master-slave 5D HRNNs.

**Theorem 4.** Suppose that Theorem 3 holds. The slave 5D HRNN (12) can achieve predefined-time synchronization with the master 5D HRNN (11) via the following controllaw:

$$\begin{aligned}u_1 &= a\hat{x}_1^3 - b\hat{x}_1^2 - ax_1^3 + bx_1^2 - e_2 + ce_3 + 3k_1s\hat{x}_5^2\hat{x}_1 - 3k_1sx_5^2x_1 \\ &\quad - \frac{2^{\eta-1}T_{\max}^2}{T_{c1}}\beta^\eta \operatorname{sign}(e_1(t)) - \frac{2^{\eta-1}T_{\max}^2}{T_{c1}}\alpha \operatorname{sign}((e_1(t))|e_1(t)|^{\gamma\eta},\end{aligned}\tag{13}$$

$$\begin{aligned}u_2 &= -he_4 - \left(\frac{2^{\eta-1}T_{\max}^2}{T_{c2}}\beta^\eta + D\right) \operatorname{sign}(e_2(t)) \\ &\quad - \frac{2^{\eta-1}T_{\max}^2}{T_{c2}}\alpha \operatorname{sign}(e_2(t))|e_2(t)|^{\gamma\eta},\end{aligned}\tag{14}$$

$$u_3 = -\frac{2^{\eta-1}T_{\max}^2}{T_{c3}}\beta^\eta \operatorname{sign}(e_3(t)) - \frac{2^{\eta-1}T_{\max}^2}{T_{c3}}\alpha \operatorname{sign}(e_3(t))|e_3(t)|^{\gamma\eta},\tag{15}$$

$$u_4 = -\frac{2^{\eta-1}T_{\max}^2}{T_{c4}}\beta^\eta \operatorname{sign}(e_4(t)) - \frac{2^{\eta-1}T_{\max}^2}{T_{c4}}\alpha \operatorname{sign}(e_4(t))|e_4(t)|^{\gamma\eta},\tag{16}$$



$$u_5 = -\frac{2^{\eta-1}T_{\max}^2}{T_{c5}}\beta^\eta \operatorname{sign}(e_5(t)) - \frac{2^{\eta-1}T_{\max}^2}{T_{c5}}\alpha \operatorname{sign}(e_5(t))|e_5(t)|^{\gamma\eta}, \quad [17]$$

$i = 1; 2; \dots; 5$ , where  $T_{ci}$  represents the predefined synchronization time of each statevariable. Then the master-slave 5D HRNNs can realize predefined-time synchronization, and the predefined time is given as

$$T_c = T_{c1} + \max\{T_{c3}, T_{c2} + T_{c4}, T_{c5}\}.$$

Proof. Define the following error system of master-slave 5D HRNNs (11) and (12):  $e_i = \hat{x}_i - x_i$ , where  $i = 1, 2, \dots, 5$ . Then we have

$$\begin{aligned} \dot{e}_1 &= -a\hat{x}_1^3 + b\hat{x}_1^2 + ax_1^3 - bx_1^2 + e_2 - ce_3 \\ &\quad - k_1de_1 - 3k_1s\hat{x}_5^2\hat{x}_1 + 3k_1sx_5^2x_1 + u_1, \\ \dot{e}_2 &= -g\hat{x}_1^2 + gx_1^2 - e_2 - he_4 + u_2 - d_{\text{dis}}, \\ \dot{e}_3 &= l[me_1 - e_3] + u_3, \\ \dot{e}_4 &= n[pe_2 - qe_4] + u_4, \\ \dot{e}_5 &= e_1 - k_2e_5 + u_5. \end{aligned} \quad (18)$$

Firstly, we consider the predefined-time synchronization between  $\hat{x}_1$  and  $x_1$ , i.e.,  $e_1$  converges to zero in predefined-time  $T_{c1}$ . Considering the candidate Lyapunov function  $V_{e_1} = \|e_1\|_1$ , then the derivative of the candidate Lyapunov function is

$$\begin{aligned} \dot{V}_{e_1} &= \operatorname{sign}(e_1(t))\dot{e}_1(t) \\ &= \operatorname{sign}(e_1(t))(-a\hat{x}_1^3 + b\hat{x}_1^2 + ax_1^3 - bx_1^2 + e_2 - ce_3 \\ &\quad - k_1de_1 - 3k_1s\hat{x}_5^2\hat{x}_1 + 3k_1sx_5^2x_1 + u_1) \\ &= \operatorname{sign}(e_1(t))\left(-k_1de_1 - \frac{2^{\eta-1}T_{\max}^2}{T_{c1}}\beta^\eta \operatorname{sign}(e_1(t))\right. \\ &\quad \left.- \frac{2^{\eta-1}T_{\max}^2}{T_{c1}}\alpha \operatorname{sign}(e_1(t))|e_1(t)|^{\gamma\eta}\right) \\ &= -k_1d|e_1(t)| - \frac{2^{\eta-1}T_{\max}^2}{T_{c1}}\beta^\eta - \frac{2^{\eta-1}T_{\max}^2}{T_{c1}}\alpha|e_1(t)|^{\gamma\eta}. \end{aligned}$$

By Lemma 4, one can obtain that

$$\begin{aligned}\dot{V}_{e_1} &\leq -\frac{2^{\eta-1}T_{\max}^2}{T_{c1}}\beta^\eta - \frac{2^{\eta-1}T_{\max}^2}{T_{c1}}\alpha|e_1(t)|^{\gamma\eta} \\ &\leq -\frac{T_{\max}^2}{T_{c1}}(2^{\eta-1}\beta^\eta + 2^{\eta-1}\alpha|e_1(t)|^{\gamma\eta}) \\ &\leq -\frac{T_{\max}^2}{T_{c1}}(\beta + \alpha|e_1(t)|^\gamma)^\eta.\end{aligned}$$

Thus, in accordance to Theorem 3, the variable  $\hat{x}_1$  and  $x_1$  can achieve predefined-timesynchronization under the controller (13) and the predefined-time is  $T_{c1}$ . Then if we plug  $e_1 = 0$  into the fifth formula of error system (18), we have

$$\dot{e}_5 = -k_2 e_5 + u_5.$$

Then we are going to implement the predefined-time synchronization between  $\hat{x}_5$  and  $x_5$ , i.e.,  $e_5$  converges to zero in predefined-time  $T_{c5}$ . Considering the candidate Lyapunov function  $V_{e_5} = \|e_5\|$ , then

$$\begin{aligned}\dot{V}_{e_5} &= \text{sign}(e_5(t))\dot{e}_5(t) \\ &= \text{sign}(e_5(t))\left(-k_2 e_5 - \frac{2^{\eta-1}T_{\max}^2}{T_{c5}}\beta^\eta \text{sign}(e_5(t))\right. \\ &\quad \left.- \frac{2^{\eta-1}T_{\max}^2}{T_{c5}}\alpha \text{sign}(e_5(t))|e_5(t)|^{\gamma\eta}\right) \\ &= -k_2|e_5| - \frac{2^{\eta-1}T_{\max}^2}{T_{c5}}\beta^\eta - \frac{2^{\eta-1}T_{\max}^2}{T_{c5}}\alpha|e_5(t)|^{\gamma\eta} \\ &\leq -\frac{T_{\max}^2}{T_{c5}}(\beta + \alpha|e_5(t)|^\gamma)^\eta.\end{aligned}$$

Thus, in accordance to Theorem 3, the variables  $\hat{x}_5$  and  $x_5$  i.e.,  $e_5$  can achieve predefined-timesynchronization under the controller (17), and the predefined-time is  $T_{c5}$ . Similarly, we have

$$\dot{e}_3 = -lme_3 + u_3.$$

Considering the candidate Lyapunov function  $V_{e_3} = \|e_3\|$ ,



$$\begin{aligned}\dot{V}_{e_3} &= \text{sign}(e_3(t))\dot{e}_3(t) = \text{sign}(e_3(t))(-lme_3 - u_3) \\ &= -lm|e_3| - \frac{2^{\eta-1}T_{\max}^2}{T_{c3}}\beta^\eta - \frac{2^{\eta-1}T_{\max}^2}{T_{c3}}\alpha|e_3(t)|^{\gamma\eta} \\ &\leq -\frac{T_{\max}^2}{T_{c3}}(\beta + \alpha|e_3(t)|^\gamma)^\eta.\end{aligned}$$

In accordance to Theorem 3, the same result can be obtained, i.e., the variables  $\hat{x}_3$  and  $x_3$  can achieve predefined-time synchronization under the controller (15), and the predefined time is  $T_{c3}$ . Similarly, we have

$$\dot{e}_2 = -e_2 - he_4 + u_2 - d_{\text{dis}}.$$

The Lyapunov function is designed as  $V_{e_2} = \|e_2\|_1$ , then

$$\begin{aligned}\dot{V}_{e_2} &= \text{sign}(e_2(t))\dot{e}_2(t) \\ &= \text{sign}(e_2(t))\left(-e_2 - he_4 + he_4 - \left(\frac{2^{\eta-1}T_{\max}^2}{T_{c2}}\beta^\eta + D\right)\text{sign}(e_2(t))\right. \\ &\quad \left.- \frac{2^{\eta-1}T_{\max}^2}{T_{c2}}\alpha\text{sign}(e_2(t))|e_2(t)|^{\gamma\eta}\right) - d_{\text{dis}} \\ &= -|e_2| - \frac{2^{\eta-1}T_{\max}^2}{T_{c2}}\beta^\eta - \frac{2^{\eta-1}T_{\max}^2}{T_{c2}}\alpha|e_2(t)|^{\gamma\eta} - (D + d_{\text{dis}}) \\ &\leq -\frac{T_{\max}^2}{T_{c2}}(\beta + \alpha|e_2(t)|^\gamma)^\eta.\end{aligned}$$

Thus, in accordance to Theorem 3, the variables  $\hat{x}_2$  and  $x_2$  can achieve predefined-time synchronization under the controller (14), and the predefined-time is  $T_{c2}$ . Then we plug into the forth formula of error system (18), and we have

$$\dot{e}_4 = -nqe_4 + u_4.$$

The Lyapunov function is designed as  $V_{e_4} = \|e_4\|_1$ , then

$$\begin{aligned}
 \dot{V}_{e_4} &= \text{sign}(e_4(t))\dot{e}_4(t) \\
 &= \text{sign}(e_4(t)) \left( -nqe_4 - \frac{2^{\eta-1}T_{\max}^2}{T_{c4}}\beta^\eta \text{sign}(e_4(t)) \right. \\
 &\quad \left. - \frac{2^{\eta-1}T_{\max}^2}{T_{c4}}\alpha \text{sign}(e_4(t))|e_4(t)|^{\gamma\eta} \right) \\
 &= -nq|e_4| - \frac{2^{\eta-1}T_{\max}^2}{T_{c4}}\beta^\eta - \frac{2^{\eta-1}T_{\max}^2}{T_{c4}}\alpha|e_4(t)|^{\gamma\eta} \\
 &\leq -\frac{T_{\max}^2}{T_{c4}}(\beta + \alpha|e_4(t)|^\gamma)^\eta.
 \end{aligned}$$

Thus, in accordance to Theorem 3, the variables  $\hat{x}_4$  and  $x_4$  can achieve predefined-time synchronization under the controller (16), and the predefined-time is  $T_{c4}$ . Then the five state variables of the 5D HRNNs all achieve predefined-time synchronization, and the synchronization time of each variable is different, i.e., the predefined synchronization time of  $\hat{x}_1$  is  $T_{c1}$ ,  $\hat{x}_2$  is  $T_{c1} + T_{c2}$ ,  $\hat{x}_3$  is  $T_{c1} + T_{c3}$ ,  $\hat{x}_4$  is  $T_{c1} + T_{c2} + T_{c4}$ , and  $\hat{x}_5$  is  $T_{c1} + T_{c5}$ . Thus, the synchronization time of the master-slave 5D HRNNs is

$$T_c = T_{c1} + \max\{T_{c3}, T_{c2} + T_{c4}, T_{c5}\}.$$

This proof is completed.

**Remark 4.** By designing the controller of each state variable of the system via backstepping, the design process can be made more simpler and convenient. We can also realize the synchronization of some of state variables of the system according to the needs of actual applications by designing the controller via backstepping.

**Remark 5.** State variables of the system can realize synchronization at different predefined time, which increases the complexity of the system. In this way, important message can be transmitted first in secure communication and different messages has its own synchronous transmission time, which increases the complexity of transmission and improves the security communication.

**Example 2.** Figures 5(a)–5(c) show the chaotic behaviors of the 5D HR neuron network (11) in a super-bursting regime projected onto the 3D subspaces of the 5D phase space:  $x_1, x_2, x_5$ -space,  $x_1, x_3, x_5$ -space,  $x_1, x_4, x_5$ -space, respectively. The constant parameters have standard values:  $a = 1.0$ ,  $b = 3.0$ ,  $c = 0.99$ ,  $f = 1.01$ ,  $g = 5.0128$ ,

$$h = 0.0278, l = 0.00215, m = 3.966, x_0 = 1.605, n = 0.0009, p = 3.0, y_0 = 1.619, q = 0.9573.$$

By simple computation,  $\alpha = 1.2$ ,  $\beta = 1.4$ ,  $\gamma = 5/6$ ,  $\eta = 2.7$ ,  $T_{c1} = 0.2$ ,  $T_{c2} = 0.2$ ,  $T_{c3} = 0.4$ ,  $T_{c4} = 0.4$ , and  $T_{c5} = 0.8$ , then the conditions of Theorem 3 hold. Parameter  $q = 0.17$ , then the

conditions of Lemma 3 hold. The master-slave 5D HRNNs are step-by-step predefined-time synchronization. For different state variables, the predefined synchronization time is different. Among them, the predefined synchronization time of  $\hat{x}_1$

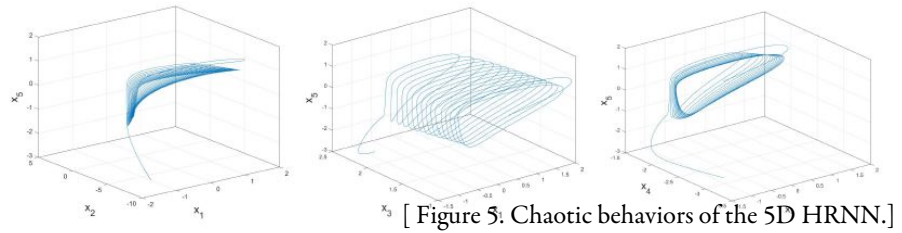
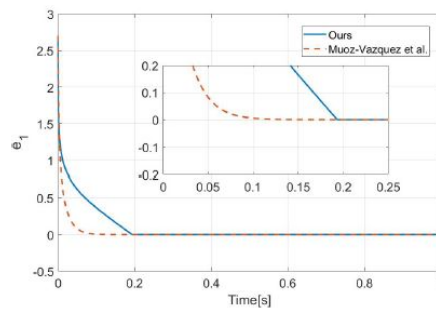
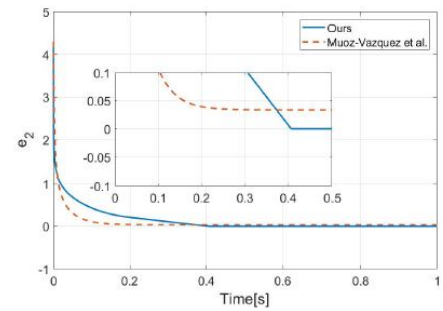


[Figure 3: Chaotic behaviors of the 5D HRNN.]

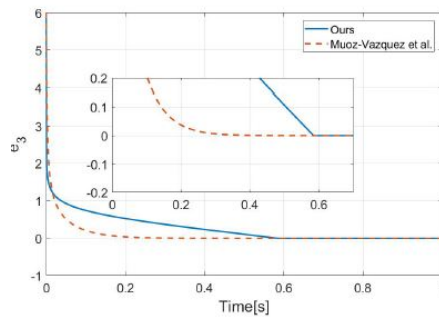
(a)  $x_1, x_2, x_5$ -space (b)  $x_1, x_3, x_5$ -space (c)  $x_1, x_4, x_5$ -space  
[Figure 9. Decrypted messages mo1 and mo2. Figure 10. Synchronization errors em1 and em2.]



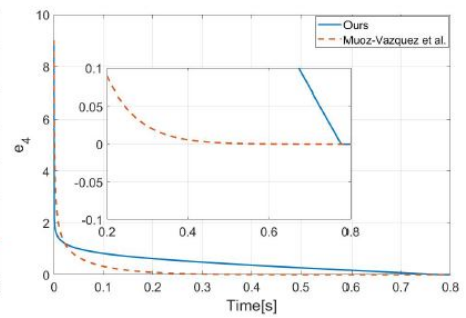
(a)  $T_{c1} = 0.2$



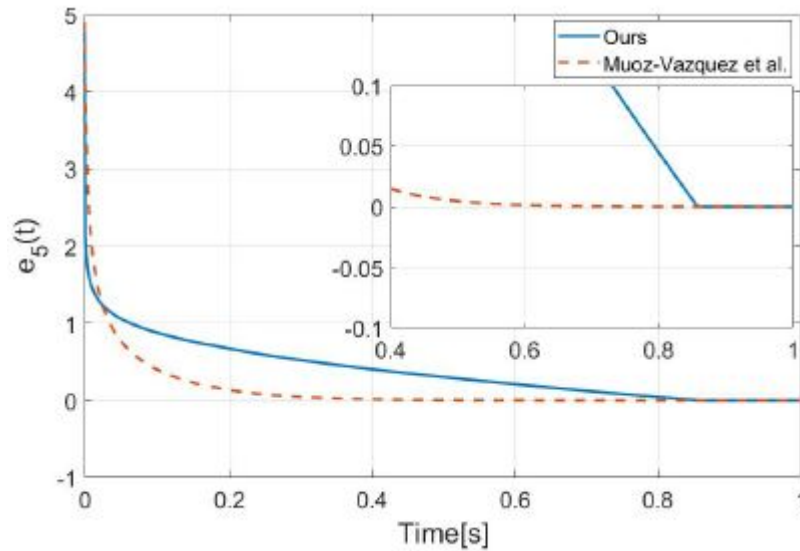
(b)  $T_{c2} = 0.2$



(c)  $T_{c3} = 0.4$



(d)  $T_{c4} = 0.4$



(e)  $T_{c5} = 0.8$

is  $T_{c1} = 0.2$ ,  $\hat{x}_2$  is  $T_{c1} + T_{c2} = 0.4$ ,  $\hat{x}_3$  is  $T_{c1} + T_{c3} = 0.6$ ,  $\hat{x}_4$  is  $T_{c1} + T_{c2} + T_{c4} = 0.8$ ,

and  $\hat{x}_5$  is  $T_{c1} + T_{c5} = 1.0$ . The simulation results are shown in Fig. 6(a) ( $e_1 = \hat{x}_1 - x_1$ ), Fig 6(b) ( $e_2 = \hat{x}_2 - x_2$ ), Fig 6(c) ( $e_3 = \hat{x}_3 - x_3$ ), Fig 6(d) ( $e_4 = \hat{x}_4 - x_4$ ), Fig 6(e) ( $e_5 = \hat{x}_5 - x_5$ ). As can be seen from Fig. 6(b), Theorem has better robustness than Lemma 3 and can effectively suppress disturbance.

## 5 Secure communication

This section proposes a secure communication algorithm based on the predefined-time synchronization of 5D HRNNs.

Example 3. By using plaintext signal, sender generates the following signals:

$$m_1 = \begin{cases} r_1(t), & 0 \leq t < 1, \\ 1.6 \sin t + 0.7 \cos(0.3t), & t \geq 1, \end{cases}$$

$$m_2 = \begin{cases} r_1(t), & 0 \leq t < 1, \\ -\sin(1.2t) + 2 \cos(3t), & t \geq 1, \end{cases}$$

where  $r1(t)$  and  $r2(t)$  denote random signals. Sender calculates the encrypted signal

$$C_1(t) = m_1(t) + x_1(t), \quad C_2(t) = m_2(t) + x_5(t).$$

Figures 7 and 8 illustrate the state trajectories of  $m_i$  and  $C_i$ , where  $i = 1, 2$ . The initial conditions of 5D HRNNs (11) and (12),  $r_1(t)$ ,  $r_2(t)$ ,  $m_1(t)$ , and  $m_2(t)$  can be known only to the sender.

Receiver receives the secret keys  $a, b, c, d, f, g, h, l, n, p, q$  and the encrypted signals  $C_1(t), C_2(t)$ . Then receiver generates the slave 5D HRNN (12). Receiver chooses the controller (13), (14), (15), (16), and (17);  $\alpha = 1.2$ ,  $\beta = 1.4$ ,  $\gamma = 5/6$ , and  $\eta = 2/7$ . According to Theorem 3, the state variables  $x_1$  and  $\hat{x}_1$ ,  $x_5$  and  $\hat{x}_5$  of master-slave 5D HRNNs can realize their own predefined-time synchronization, and their predefined synchronization time is  $T_{c1} = 2$  and  $T_{c5} = 8$ , respectively. Figures 9 and 10 illustrate the receiver decrypted the encrypted messages by calculating  $m_{oi} = C_i - \hat{x}_i$  and the message error  $e_{mi} = m_{oi} - m_i$ . As can be seen from Fig. 10, message  $m_1$  achieved accurate transmission within  $T_{c1} = 2$  s, and message  $m^2$  achieved accurate transmission within  $T_{c1} + T_{c5} = 10$  s.

In this way, different messages have its own synchronous transmission time, and the receiver can get accurate message after the predefined time, which increases the complexity of transmission and improves the security communication.

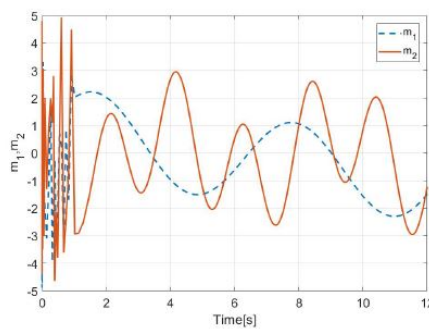


Figure 7. Plaintext messages  $m_1$  and  $m_2$ .

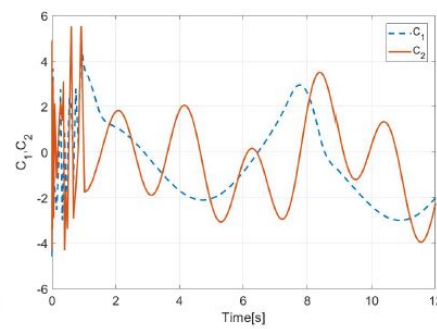


Figure 8. Encrypted signals  $C_1$  and  $C_2$ .

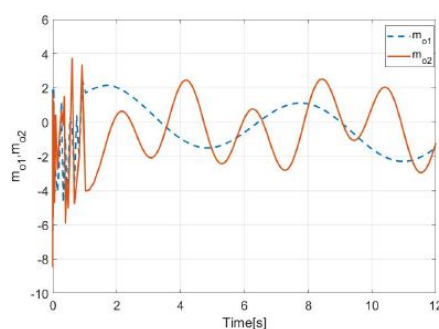


Figure 9. Decrypted messages  $m_{o1}$  and  $m_{o2}$ .

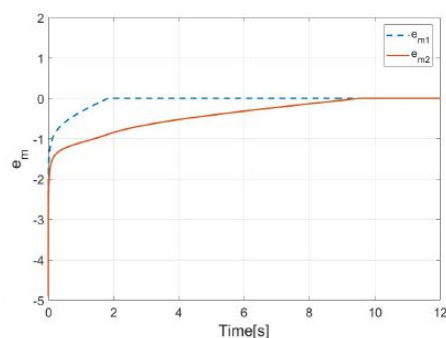


Figure 10. Synchronization errors  $e_{m1}$  and  $e_{m2}$ .

## 6 Conclusion

the predefined-time synchronization of 5D HRNNs in which the synchronization time of each state variable of the master-slave 5D HRNNs is different and can be defined in advance. To show the



applicability of the theoretical results obtained, the designed predefined-time controller has been applied to secure communication to realize asynchronous communication of multiple messages. In the future research work, we will continue to study the predefined-time secure communication under the influence of disturbances and apply it to other fields, such as discrete-time Boolean control networks, fuzzy sets, and fractional order neural networks.

## Acknowledgments

The author thanks the anonymous reviewers for their insightful suggestions, which improved this work significantly

## References

- 1 S. Aadithiyan, R. Raja, Q. Zhu, J. Alzabut, C.P. Lim, Exponential synchronization of nonlinear multi-weighted complex dynamic networks with hybrid time varying delays, *Neural Process. Lett.*, 53(1035–1063), 2021, <https://doi.org/10.1007/s11063-021-10428-7>.
- 2I. Ahmad, A Lyapunov-based direct adaptive controller for the suppression and synchronization of a perturbed nuclear spin generator chaotic system, *Appl. Math. Comput.*, 395:125858, 2020, <https://doi.org/10.1016/j.amc.2020.125858>. <https://www.journals.vu.lt/nonlinear-analysis>
- 3I. Ahmad, A.B. Saaban, A.B. Ibrahim, S. Al-Hadhrami, M. Shahzad, S.H. Al-Mahrouqi, A research on adaptive control to stabilize and synchronize a hyperchaotic system with uncertain parameters., *Int. J. Optim. Control, Theor. Appl. (IJOCTA)*, 5(2):51-62, 2015, <https://doi.org/10.11121/ijocta.01.2015.00238>.
- 4I. Ahmad, M. Shafiq, A generalized analytical approach for the synchronization of multiple chaotic systems in the finite time, *Arab. J. Sci. Eng.*, 45(3):2297–2315, 2020, <https://doi.org/10.1007/s13369-019-04304-9>.
- 5I. Ahmad, M. Shafiq, Oscillation free robust adaptive synchronization of chaotic systems with parametric uncertainties, *Trans. Inst. Meas. Control*, 42(11):1977–1996, 2020, <https://doi.org/10.1177/0142331220903668>.
- 6I. Ahmad, M. Shafiq, M. Shahzad, Global finite-time multi-switching synchronization of externally perturbed chaotic oscillators, *Circuits Syst. Signal Process.*, 37:5253–5278, 2018, <https://doi.org/10.1007/s00034-018-0826-4>.
- 7C. Chen, L. Li, H. Peng, Y. Yang, L. Mi, L. Wang, A new fixed-time stability theorem and its application to the synchronization control of memristive neural networks, *Neurocomputing*, 349:290–300, 2019, <https://doi.org/10.1016/j.neucom.2019.03.040>.
- 8K. Ding, Q. Zhu, A note on sampled-data synchronization of memristor networks subject to actuator failures and two different activations, *IEEE Trans. Circuits Syst. II Express Briefs*, 68(6):2097–2101, 2021, <https://doi.org/10.1109/TCSII.2020.3045172>.

- 9S. Dubuc, I. Kagabo, Handbook of mathematical functions with formulas, RAIRO, Oper. Res., 40(1):1–17, 2006, <https://doi.org/10.1051/ro:2006011>.
- 10J.L. Hindmarsh, R.M. Rose, A model of the nerve impulse using two first-order differential equations, *Nature*, 296(5853):162–164, 1982, <https://doi.org/10.1038/296162a0>.
- 11A.L. Hodgkin, A.F. Huxley, A quantitative description of membrane current and its application to conduction and excitation in nerve, *J. Physiol.*, 117(4):500–544, 1952, <https://doi.org/10.1113/jphysiol.1952.sp004764>.
- 12C. Hu, J. Yu, Z. Chen, H. Jiang, T. Huang, Fixed-time stability of dynamical systems and fixedtime synchronization of coupled discontinuous neural networks, *Neural Netw.*, 89:74–83, 2017, <https://doi.org/10.1016/j.neunet.2017.02.001>.
- 13 E. Jiménez-Rodríguez, J.D. Sánchez-Torres, A.G. Loukianov, On optimal predefined-time stabilization, *Int. J. Robust Nonlinear Control*, 27(17):3620–3642, 2017, <https://doi.org/10.1002/rnc.3757>.
- 14 F. Kong, Q. Zhu, New fixed-time synchronization control of discontinuous inertial neural networks via indefinite lyapunov-krasovskii functional method, *Int. J. Robust Nonlinear Control*, 31:471–495, 2021, <https://doi.org/10.1002/rnc.5297>.
- 15 F. Kong, Q. Zhu, T. Huang, New fixed-time stability lemmas and applications to the discontinuous fuzzy inertial neural networks, *IEEE Trans. Fuzzy Syst.*, 29(12):3711–3722, 2021, <https://doi.org/10.1109/TFUZZ.2020.3026030>.
- 16 F. Kong, Q. Zhu, R. Sakthivel, A. Mohammadzadeh, Fixed-time synchronization analysis for discontinuous fuzzy inertial neural networks with parameter uncertainties, *Neurocomputing*, 422:295–313, 2021, <https://doi.org/10.1016/j.neucom.2020.09.014>.
- 17 M. Kuczma, A. Gilányi, An Introduction to the Theory of Functional Equations and Inequalities, Birkhäuser, Basel, 2009. *Nonlinear Anal. Model. Control*, 27(4):630–649, 2022.
- 18 L. Lin, Predefined-time antisynchronization of two different chaotic neural netw., *Complexity*, 2020:7476250, 2020, <https://doi.org/10.1155/2020/7476250>.
- 19 L. Lin, P.Wu, Y. Chen, B. He, Enhancing the settling time estimation of fixed-time stability and applying it to the predefined-time synchronization of delayed memristive neural networks with external unknown disturbance, *Chaos*, 30(8):083110, 2020, <https://doi.org/10.1063/5.0010145>.
- 20 S.A. Malik, A.H. Mir, Synchronization of Hindmarsh Rose neurons, *Neural Netw.*, 123:372–380, 2020, <https://doi.org/10.1016/j.neunet.2019.11.024>.
- 21 E.B. Megam Ngouonkadi, H.B. Fotsin, P. Louodop Fotso, V. Kamdoun Tamba, H.A. Cerdeira, Bifurcations and multistability in the extended hindmarsh–Rose neuronal oscillator, *Chaos Solitons Fractals*, 85:151–163, 2016, <https://doi.org/10.1016/j.chaos.2016.02.001>.
- 22 A.J. Muñoz-Vázquez, J.D. Sánchez-Torres, E. Jiménez-Rodríguez, A.G. Loukianov, Predefined-time robust stabilization of robotic manipulators,



- IEEE/ASME Trans. Mechatron., 24(3):1033–1040, 2019, <https://doi.org/10.1109/TMECH.2019.2906289>.
- 23 A.J. Muñoz-Vázquez, J.D. Sánchez Torres, S. Gutiérrez-Alcalá, E. Jiménez-Rodríguez, A.G. Loukianov, Predefined-time robust contour tracking of robotic manipulators, J. Franklin Inst., 356(5):2709–2722, 2019, <https://doi.org/10.1016/j.jfranklin.2019.01.041>.
- 24 A.J. Muñoz-Vázquez, J.D. Sánchez Torres, C.A.A. Gijón, Single-channel predefined-time synchronisation of chaotic systems, Asian J. Control, pp. 190–198, 2021, <https://doi.org/10.1002/asjc.2234>.
- 25 A. Polyakov, Nonlinear feedback design for fixed-time stabilization of linear control systems, IEEE Trans. Autom. Control, 57(8):2106–2110, 2012, <https://doi.org/10.1109/TAC.2011.2179869>.
- 26 J.D. Sánchez-Torres, D. Gómez-Gutiérrez, E. López, A.G. Loukianov, A class of predefined-time stable dynamical systems, IMA J. Math. Control Inf., 35(Suppl.\_1):i1–i29, 2018, <https://doi.org/10.1093/imamci/dnx004>.
- 27 J.D. Sánchez-Torres, E.N. Sanchez, A.G. Loukianov, A discontinuous recurrent neural network with predefined time convergence for solution of linear programming, in 2014 IEEE Symposium on Swarm Intelligence, IEEE, Piscataway, NJ, 2014, pp. 1–5, <https://doi.org/10.1109/SIS.2014.7011799>.
- 28 M. Storace, D. Linaro, E. D. Lange, The hindmarsh–Rose neuron model: Bifurcation analysis and piecewise-linear approximations, Chaos, 18(3):033128, 2008, <https://doi.org/10.1063/1.2975967>.
- 29 K. Usha, P.A. Subha, Hindmarsh–Rose neuron model with memristors, Biosystems, 178:1–9, 2019, <https://doi.org/10.1016/j.biosystems.2019.01.005>.
- 30 K.M. Wouapi, B.H. Fotsin, F.P. Louodop, K.F. Feudjio, T.H. Djeudjo, Various firing activities and finite-time synchronization of an improved Hindmarsh–Rose neuron model under electric field effect, Cognitive Neurodynamics, 14:375–397, 2020, <https://doi.org/10.1007/s11571-020-09570-0>.
- 31 M.E. Yamakou, Chaotic synchronization of memristive neurons: Lyapunov function versus Hamilton function, Nonlinear Dyn., 101(1):487–500, 2020, <https://doi.org/10.1007/s11071-020-05715-2>. <https://www.journals.vu.lt/nonlinear-analysis> Predefined-time synchronization of 5D Hindmarsh–Rose neuron networks 649
- 32 X. Yi, L. Ren, Z. Zhang, New criteria on global asymptotic synchronization of Duffing-type oscillator system, Nonlinear Anal. Model. Control, 25(3):378–399, 2020, <https://doi.org/10.15388/namc.2020.25.16656>.
- 33 Q. Zhu, J. Cao, pth moment exponential synchronization for stochastic delayed Cohen–Grossberg neural networks with Markovian switching, Nonlinear Dyn., 67(1):829–845, 2012, <https://doi.org/10.1007/s11071-011-0029-z>. Nonlinear Anal. Model. Control, 27(4):630–649, 2022